# State of the art in silicon immersed gratings for space

Aaldert van Amerongen[1], Hélène Krol[2], Catherine Grèzes-Besset[2], Tonny Coppens[1], Ianjit Bhatti[3], Dan Lobb[3], Bram Hardenbol[4], Ruud Hoogeveen[1]

[1]SRON Netherlands Institute for Space Research, Sorbonnelaan 2, 3584 CA Utrecht, The Netherlands

[2]CILAS Etablissement de Marseille, ZI St Mitre - Av. de la Roche Fourcade, 13400 Aubagne, France

[3]Surrey Satellite Technology Ltd., Rayleigh House, 1 Bat and Ball Road, Sevenoaks, Kent, TN14 5LJ, United Kingdom

[4]TNO Technical Sciences, Stieltjesweg 1, 2628 CK, Delft, The Netherlands

*Abstract*— **We present the status of our immersed diffraction grating technology, as developed at SRON and of their multilayer optical coatings as developed at CILAS. Immersion means that diffraction takes place inside the medium, in our case silicon. The high refractive index of the silicon medium boosts the resolution and the dispersion. Ultimate control over the groove geometry yields high efficiency and polarization control. Together, these aspects lead to a huge reduction in spectrometer volume. This has opened new avenues for the design of spectrometers operating in the short-wave-infrared wavelength band. Immersed grating technology for space application was initially developed by SRON and TNO for the short-wave-infrared channel of TROPOMI, built under the responsibility of SSTL. This space spectrometer will be launched on ESA's Sentinel 5 Precursor mission in 2015 to monitor pollution and climate gases in the Earth atmosphere. The TROPOMI immersed grating flight model has technology readiness level 8. In this program CILAS has qualified and implemented two optical coatings: first, an anti-reflection coating on the entrance and exit facet of the immersed grating prism, which reaches a very low value of reflectivity for a wide angular range of incidence of the transmitted light; second, a metal-dielectric absorbing coating for the passive facet of the prism to eliminate stray light inside the silicon prism. Dual Ion Beam Sputtering technology with in-situ visible and infrared optical monitoring guarantees the production of coatings which are nearly insensitive to temperature and atmospheric conditions. Spectral measurements taken at extreme temperature and humidity conditions show the reliability of these multi-dielectric and metal-dielectric functions for space environment. As part of our continuous improvement program we are presently developing new grating technology for future missions, hereby expanding the spectral range, the blaze angles and grating size, while optimizing performance parameters like stray light and wavefront error. The program aims to reach a technology readiness level of 5 for the newly developed technologies by the end of 2012. An outlook will be presented.**

***Immersed grating, spectrometer, silicon, multilayer coatings, metal-dielectric absorbers, Dual Ion Beam Sputtering, stray light, cryogenic qualification***

## I. INTRODUCTION

Silicon immersed gratings enable a huge decrease in spectrometer size in the short-wave-infrared (SWIR) wavelength range because diffraction takes place inside the high-index medium. This volume reduction is especially interesting for application in space where Earth-observing spectrometers collect reflected sunlight to monitor air pollution and climate gases. For climate research the main gases of interest are CO2, CH4 and H2O and HDO, all observable in the 1.6 - 2.4 micrometer range, specifically in three bands that we will refer to as: SWIR1 at 1.6 micrometer (CO2, CH4), SWIR 2 at 2.0 micrometer (CO2, H2O) and SWIR 3 at 2.3 micrometer (CH4, H2O, HDO). The pollution gas CO is also observable in the SWIR-3 band.

Immersed gratings have been often proposed. We have recently developed the first IG to fly in space for the TROPOMI instrument to be launched by ESA on the Sentinel 5 precursor mission. The TROPOMI instrument consists of a UV-VIS-NIR spectrometer build by TNO Science and Industry (the Netherlands) and a SWIR spectrometer build by SSTL (UK). The prime contractor for TROPOMI is Dutch Space (the Netherlands), [1]. SRON has manufactured and delivered a set of flightworthy gratings to SSTL. Each grating has two highly specialized coatings developed by CILAS (F).

In Section II we describe the grating design and manufacturing. Test results are given in Section III. SRON develops gratings in close collaboration with its partners TNO and Philips Innovation Services (the Netherlands), coatings are developed in collaboration with CILAS. We have, over the past seven years, become increasingly fast in developing new grating concepts. Ongoing developments to answer future needs are discussed in Section IV. We conclude in Section V.

## II. TROPOMI DESIGN AND MANUFACTURING

We will describe here the IG design, the production flow and the performance results for the TROPOMI flight model gratings. To give some perspective a short description of the SWIR spectrometer design is given.

### *A. Spectrometer design*

The status of the TROPOMI instrument is discussed in detail in [2]. On TROPOMI the SWIR and UVN spectrometers share a common telescope. Fig. 1 (Top) shows the layout of the

This work was made possible by NSO grant PEP11012 and with funding by the European Union.

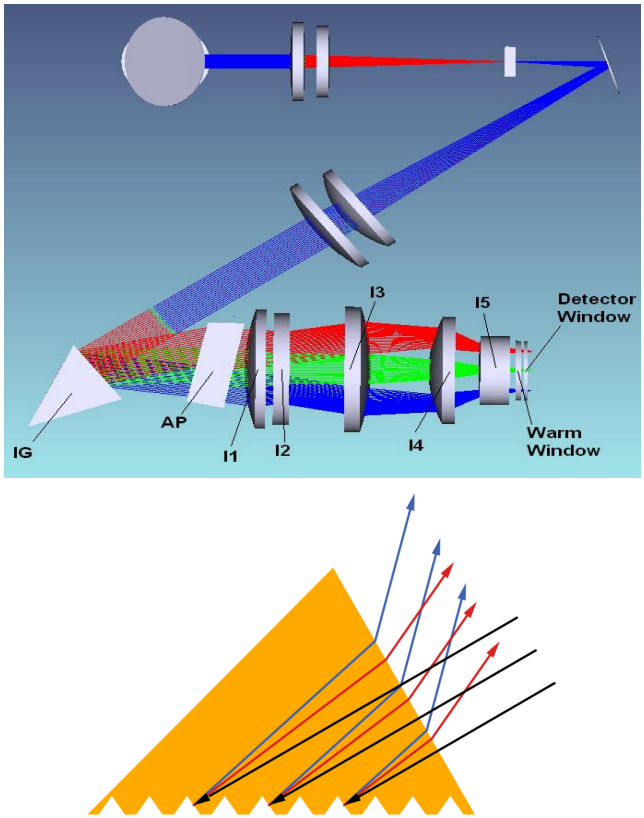


Figure 1 Top: optical layout of the TROPOMI SWIR Spectrometer including the Immersed grating (IG), an anamorphic prism (AP), camera-objective lenses l1-l5, and detector windows. Bottom: Schematic Immersed grating with V-grooves. Incoming rays in black, dispersed light in red and blue.

SWIR spectrometer. A relayed image of the TROPOMI telescope input pupil is provided at the interface to the SWIR module. A SWIR telescope comprising a silicon germanium doublet forms an image of the ground on a SWIR slit. The slit is manufactured on a silicon prism using photo lithographic methods. A second silicon germanium doublet collimates light from the slit into the immersed grating (IG). A five element imaging lens (l1 - l5) comprising silicon and germanium elements forms a spectrally dispersed image of the slit on a MCT detector. An anamorphic prism (AP) is included between the immersed grating and the imaging lens and this provides fine alignment adjustment for co-registration requirements.

### *B. Grating design*

Fig. 1 (Bottom) shows the IG schematically, with the incoming rays in black and dispersed rays in blue and red. The grating surface shows the characteristic V-grooves (not to scale) that arise from our etching technique; grooves are etched along a specific crystallographic direction of the mono-crystalline silicon grating material. This method results in a controlled blaze angle close to 55°, and smooth groove surfaces. The grating period is 2500 nm corresponding to 400 lines per millimeter. The flat parts in the plane of the grating, between the grooves are 800 nm wide. The grating is used in order -6. The grating facet has a reflective coating. The angle between the grating entrance facet and grating facet is 60 degrees. The incoming beam is at normal incidence with the entrance facet. This facet has a multi-dielectric AR coating that is described in Section IIIC.

### *C. Mounting the grating*

The immersed grating is a single crystal of silicon with a grating surface etched onto one face. The operational temperature of the optical bench is 200 K. The immersed grating is mounted in a monolithic titanium alloy structure (Fig. 2); it is held into the structure by epoxy adhesive (Masterbond EP21TCHT-1). The epoxy adhesive is contained in recesses within invar buttons to control the bond line thickness. Invar is used at the adhesive interface as its coefficient of thermal expansion (CTE) is a good match to that of the silicon of the immersed grating over the required temperature range. This will limit the stress induced birefringence and also ensures that stresses in the adhesive are kept to a minimum. Due to the CTE difference between titanium alloy and the silicon prism, flexure sections are required in the mounting structure to compensate for displacements at operating temperature. The invar buttons are therefore mounted into flexure arms which feature a thin blade section to compensate for displacements across the prism and folded flexure spring sections to compensate for further displacements.

### *D. Production and verification*

The manufacturing flow of the IG's can be summarized as follows: First, cylindrical ultrapure silicon substrates of 100 mm diameter and 50 mm high are procured. Second, grating grooves are patterned and etched on a surface using UV lithography followed by reactive ion etching to open up a masking layer and subsequent anisotropic chemical wet etching of the V-grooves. Details of the lithography and etching are given in [3], see also [4]. For the lithography, we have used a mask with the grating template that was made by laser holography. Holography does not suffer from stitching errors often seen in masks that are written in a stepping mode with laser or e-Beam writers. However, any wave front aberrations in the illumination setup are recorded in the hologram and transferred to the final grating. Dedicated equipment was developed at SRON to work with the extraordinarily thick substrates. Third, the grating surface is coated with an aluminium reflective coating and a ceramic protection layer. In step four, at TNO, a prism shape is carved out of the substrate using milling followed by manual grinding. The facets are then polished to below 63 nm peak-to-valley flatness and below 1 nm rms roughness. The fifth and final manufacturing step is carried out by CILAS, where an AR-coating and an absorbing coating are deposited on two of the prism faces.

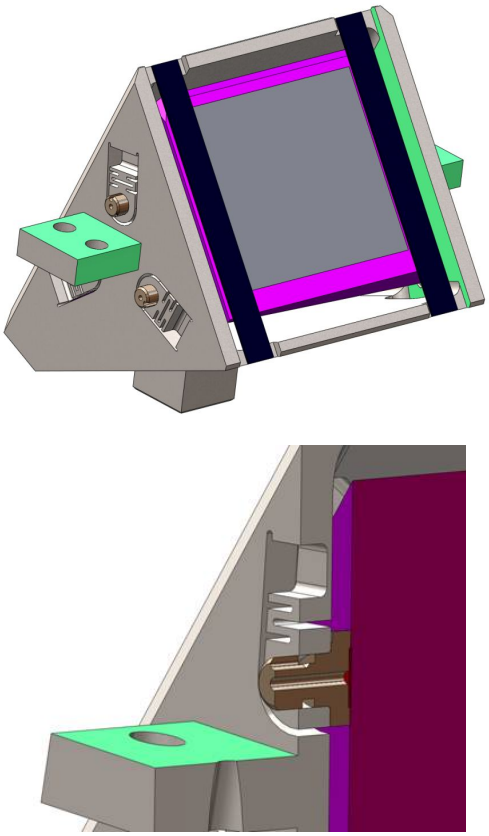

Figure 2 Mounting the immersed grating. Top: The immersed grating prism (purple) is mounted in a monolithic titanium alloy structure (grey); it is held into the structure by epoxy adhesive. Invar is used at the adhesive interface. Bottom: zoom of the mounting structure showing an invar button (brown) mounted in a flexure spring section of the titanium structure.

We decided to make an initial breadboard model (BBM) grating to bridge the development phase to the production phase of the TROPOMI engineering/qualification model and the flight and spare models (EQM, FM, FS). The EQM model will be used at SSTL to develop and qualify the mounting structure. Manufacturing of one model takes eight months. To complete four models in the 18 month timeframe of the contract the models were developed partly in parallel completing a new model every three months or so. This implies that lessons learned in the BBM model had to be incorporated in the project while the production chain was already running at the three manufacturing sites: SRON, TNO and CILAS. To get this to work, simultaneous engineering was needed. This meant that from the start of the project at all three sites processes were developed in parallel, based on initial parameters that were well tuned between the three teams. Subsequently, while the chain was running, continuous coordination between the efforts at the three teams and quick problem solving and implementation of changes was essential.

During production and partly after completion verification of the products was done as follows. At arrival we carefully characterize the substrates on flatness, roughness, crystal orientation, and sub-surface damage. We then start the critical steps of the lithography and etching, monitored with SEM

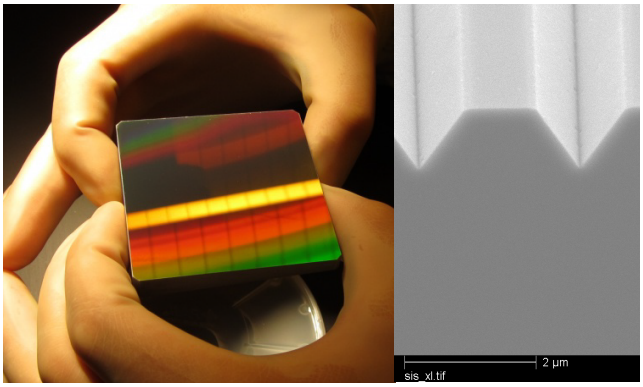


Figure 3 Left: The FM immersed grating during final inspection. Right: Scanning electron micrograph of V-groove grating profile on a test piece.

inspections. The reflective coating stack is tested according to the ISO 9211-3 standard following humidity (48h, 95% humidity, 40 °C) and thermal cycling (-80 °C; +50 °C; 20 cycles) tests. The shaping of the prism is verified using optical interferometry. The verification at CILAS is also based on ISO 9211-3 as described in Section IIIC. Finally, SRON performs a series of tests to characterize the stray light and efficiency performance. Results are discussed in Section III.

## III. TROPOMI RESULTS

The manufacturing and test of the IGs was completed in July 2012. The FM and spare gratings are fully compliant with the opto-mechanical specifications. The wave front error is 0.6 µm rms and can be reduced to 0.3 µm rms with focus correction. The wave-front error has many contributions (surface unflatness, lithography non-uniformity, mask imperfections). In our case, the holographically-produced mask is the largest contributor. In future projects there is room for improvement. The FM grating during final inspection is shown in Fig. 3 (Left). An electron micrograph of the typical V-groove grating profile on a test piece is shown in Fig. 3 (Right). Optical performance on stray light, efficiency and coating reflectivity is detailed below.

### *A. Stray light performance*

We have used a compact spectrometer that is equipped with an off-the-shelf Sofradir Mars SWIR detector to characterize the stray-light performance. A DFB laser (Nanoplus at 2323 nm) is used as a single-frequency light source. We collect 2D spectral images. Horizontally, the spectral range from 2318 nm to 2353 nm is projected onto 320 columns. This corresponds to an angular range exiting the grating of ± 5°. Vertically, a field of ± 4° is projected onto 256 rows. Cuts in horizontal and vertical direction are displayed in Fig. 4 on a logarithmic intensity scale. The maximum intensity is normalized to 1. The stray light level drops relatively quickly to the $10^{-4}$ level where it exhibits a shoulder. Further from the peak the light intensity drops to the $10^{-6}$ level. The measurement in spectral direction in Fig. 4 is limited by a regular pattern of side modes of the DFB laser at the $10^{-5}$ level, in line with the manufacturer specification of a side mode rejection ratio of 48 dB. The used spectrometer is known to suffer from significant reflections on the order of $10^{-3}$. The reflections originate primarily at the

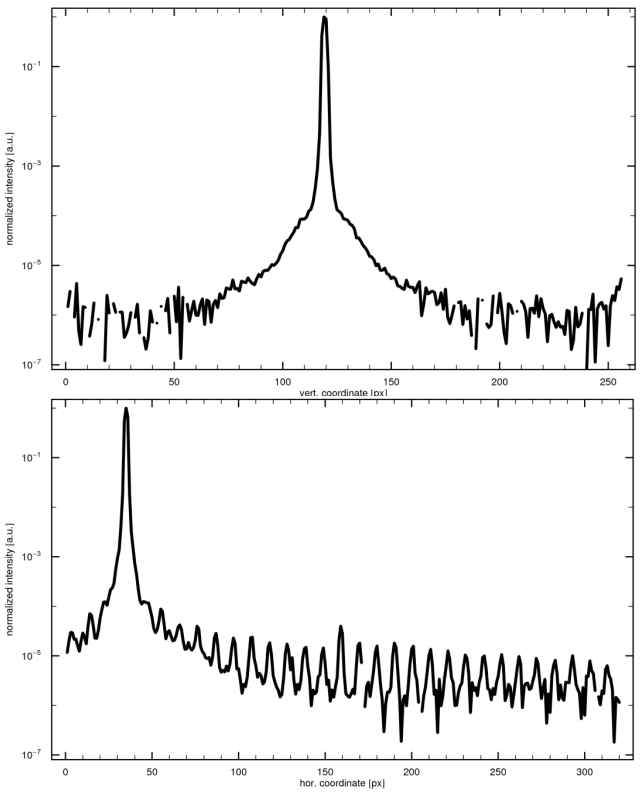


Figure 4 FM grating stray light, in across-spectral direction (Top) and in spectral direction (Bottom). The regular array of peaks at the $10^{-5}$ level stems from laser side-modes, the actual stray-light level is $10^{-6}$.

detector surface, in combination with the detector window. Both are not optimized for the applied wavelength. Therefore, final stray light performance will be assessed in more detail only after integration of the IG in the final SWIR optical bench.

### *B. Efficiency performance*

Grating-efficiency measurements are performed with a Perkin-Elmer lambda 950 photo-spectrometer at TNO. The photo-spectrometer is equipped with an Absolute Reflectance/Transmittance Analyzer (ARTA) add-on from OMT solutions (The Netherlands). The ARTA is a stepper motor driven goniometer tool that uses an integrating sphere as detector. It is capable of recording transmittance and reflectance spectra as a function of the angle of incidence and polarization. Fig.5 shows the measured efficiency (continuous lines) compared to results from simulation with the PC-Grate software package. Polarizations TM and TE are shown in grey and black respectively. The operational wavelength band is shaded. The average efficiency over the band is 63% and the polarization 9%. The agreement between simulation and measurement is striking. In other grating models we have measured efficiencies maximally 5% lower than simulated. We ascribe the discrepancies to tolerances in the manufacturing of the groove widths.

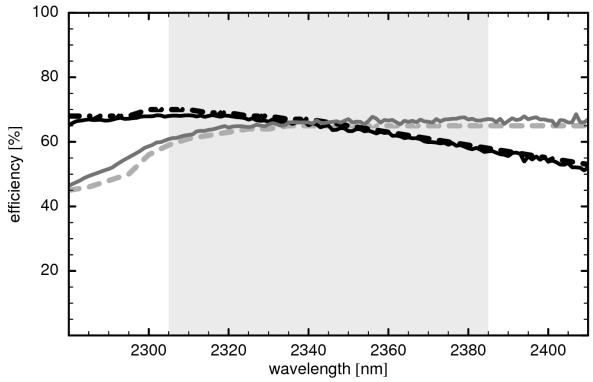


Figure 5 FM grating efficiency with TM polarization in Grey and TE polarization in black. Simulated data are dashed, measured data continuous.

### *C. Coating design and performance*

Two specific coatings for the IG prisms have been implemented and qualified by CILAS. On the entrance facet of the immersed grating prism, the antireflection coating is specified with a low value of reflectivity in the infrared spectral range: R<0.5% for 2280 nm to 2410 nm at 0° AoI, R<0.2% for 2431 nm at 14° AoI and for 2385 nm at 25° AoI, and R<0.5% for 2305nm at 47° AoI. On the passive facet of the immersed grating prism, a metal-dielectric absorbing coating has been designed to eliminate stray light inside the silicon prism. For this coating the requirement is R<1.5% for 2280nm to 2410nm at 0° to 30° AoI in the silicon prism medium. The requirement and simulated spectral performance of both coatings are given in Fig. 6 (Top). The severe operational conditions of the IG prism (temperature: - 83 °C to -63 °C and space vacuum) requires a dense coating deposition technique in order to be insensitive to temperature and atmospheric conditions. Therefore, the two coatings have been developed on breadboard and qualification models and realized on flight models using Dual Ion Beam Sputtering (DIBS). The deposition process is aided by a real-time in-situ visible and infrared optical monitoring system [5]. Measured spectral performances of both coatings are given in Fig. 6 (Bottom). A picture of the FM prism with the two coatings is shown in Fig. 7.

Environmental and durability qualification tests have been conducted on witness samples and on the EQM model. Tests were performed according to the following list:

- Thermal cycling: 20 cycles -80 / +50 °C with 2°/min slope and 1 hour min/max stage at ambient pressure and under nitrogen atmosphere.
- Humidity qualification: 48 hours exposure to 40°C and 95% humidity.
- Adhesion, according to ISO 9211-3, test 02, level 02
- Abrasion, according to ISO 9211-3, test 01, level 01

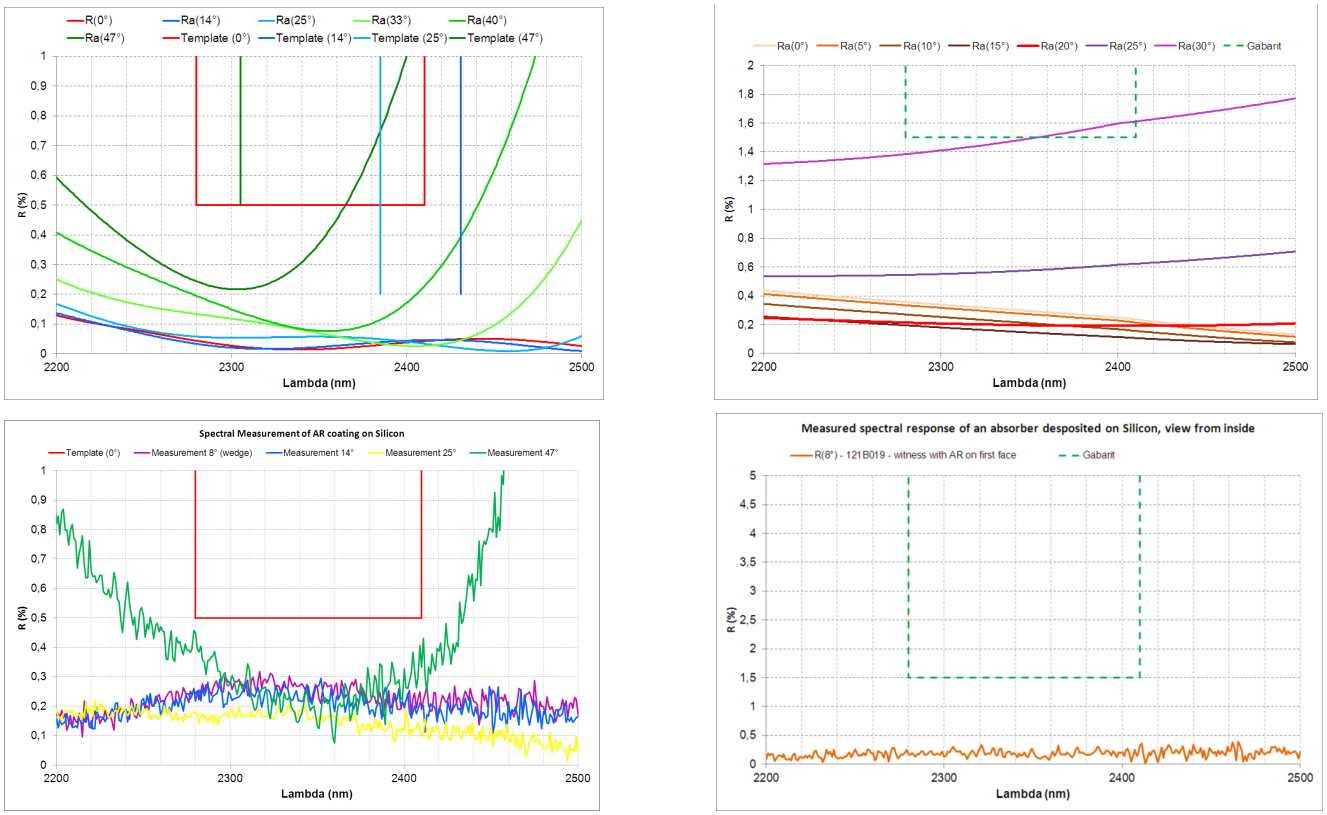


Figure 6 Simulated spectral performance of the antireflection coating for various AoI (Top Left), and of the absorbing coating (Top Right). Measured spectral performance of the antireflection coating for various AoI (Lower Left) and for the absorbing coating for 8 degrees AoI (Lower Right).

All tests were passed successfully. Spectral measurements and the results of the qualification tests show the reliability of these multi-dielectric and metal-dielectric functions for space environment. Radiation hardness was demonstrated using data taken earlier in the context of a pre-development program for ESA. Here radiation tests were performed on the same type of coatings (same materials, same coating machine), also deposited on silicon. Samples were irradiated with protons with energy of up to 40 MeV, and a flux of $2\times10^{10}$ protons/cm$^2$, and with Gamma radiation with 60 krads total radiation dose. No degradation of the optical performances of the coatings under radiation has been measured.

## IV. Ongoing Developments

The increasing awareness of the changing composition of trace gases in the Earth atmosphere has resulted in a worldwide interest to monitor the chemical composition from space. In Europe, the USA and Asia initiatives are developed for future missions that include spectrometry in the SWIR wavelength range. As we have shown with the TROPOMI SWIR results, IG-based spectrometers pose an attractive alternative to existing solutions. However, the demand for higher spectrographic and geographic accuracy leads to required IG-performance beyond the current state-of-the-art. In the following, we will briefly touch on future needs and the developments that we are currently working on.

### A. *Needs for the future*

To extend the measurement capabilities and the range of observable trace gases, there is a need for gratings, not only in the SWIR 3 wavelength band, but also for SWIR 1 and SWIR 2. Additionally, these future applications ask for an unpolarized efficiency larger than 60 %, while the polarization remains, typically, below 10%. Further, low stray light and improved WFE performance are required. To answer these needs we develop along the following routes:

### B. *Bonding*

The most important improvement with respect to the TROPOMI process is that we now also pattern wafers with standard thickness instead of the odd 50 mm thick substrates. These wafers are later contact bonded to a prism, followed by a thermal fusing step. Working on wafers of standard thickness allows for much faster improvement cycles and the use of standard techniques and equipment from the semiconductor industry. We can now, for example, use advanced equipment and expertise available in the labs of Philips Innovation Services (PINS). The result is better performance at decreased cost: we have increased the process batch size while decreasing the processing time. Using wafers with standard thickness was not feasible before because their thickness is not constant enough resulting in a large wave-front error in the immersed gratings. The introduction of a dedicated polish step to reduce the thickness variation opened the route to wafer-to-prism bonding.

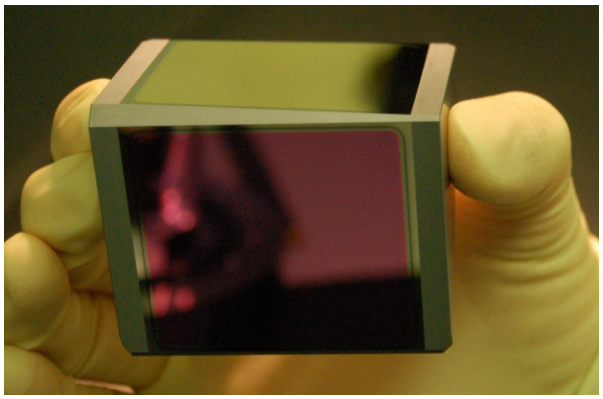

Figure 7 IG Flight Model with its absorbing coating (top) and AR-coating (bottom).

For example, for a ground-based SWIR-MIR spectrometer SRON and partners develop an immersed grating with a grating surface area of 80 x 140 mm [4]. Here, the grating wafer and prism will be produced separately and contact bonded followed by thermal fusing at high temperature.

### C. *Blazed gratings*

SRON, SSTL and TNO are involved in a pre-development program for ESA missions, partly funded by the Dutch government. In this program we will develop immersed gratings with blaze angles other than the current 55°. This hugely widens the parameter space for the design of high-efficiency gratings. To this end, lithography will be done on wafers that are cut at an angle with respect to the standard <100> crystal orientation, resulting in asymmetric V-grooves. Subsequently, the wafer will be cut and contact bonded to a prism followed by thermal fusing at high temperature. The wafer size will be 100 mm diameter.

### D. *High line density*

In the same program, a 100 mm size regular wafer will be patterned with gratings with a period of ~430 nm, equivalent to 2325 l/mm. When contact bonded and fused to a prism, these immersed gratings operate in first diffraction order resulting in higher efficiency and a lower level of stray light.

### E. *Coatings for SWIR 1 and SWIR 2*

Preliminary studies are conducted by CILAS to evaluate spectral performances of anti-reflection coatings in the other SWIR wavelength bands of interest for trace gas monitoring: 1.6 μm and 2.0 μm. The same production process and materials can be used to reach similarly low reflectivity, i.e. below 0.5% for a wide range of angles of incidence [0°, -50°] over the scientifically relevant wavelength range.

## V. CONCLUSIONS

We have manufactured and tested immersed diffraction gratings for the TROPOMI SWIR spectrometer. The optical performance is compliant with the requirements. We have developed and tested specific absorbing and AR-coatings with low reflectivity. The coatings survive extensive thermal cycling and humidity conditions.

We have presented an outlook to future developments in IGs encompassing the complete set of SWIR wavelength bands at 1.6, 2.0 and 2.3 micrometers. We develop wafer to prism bonding allowing for immersed-grating sizes well beyond 10 cm, gratings with arbitrary blaze angles and high-line density first-order gratings.

## ACKNOWLEDGMENT

We like to acknowledge Huib Visser who proposed the presented IGs, and our partners at PINS: Govert Nieuwland and team. Advice of Dan Jaffe is highly appreciated.

## REFERENCES

[1] Johan de Vries, Robert Voors, Gerard Otter, Nick van der Valk, Ilse Aben, Ruud Hoogeveen, Ralph Snel, Quintus Kleipool and Pepijn Veefkind, “PDR status for TROPOMI, the Sentinel 5 precursor instrument for air quality and climate observations,” Proc. SPIE 8176, 817609 (2011).

[2] Robert Voors, Johan de Vries, Marc Oort, Nick van der Valk, Ilse Aben, Pepijn Veefkind, Ianjit Bhatti, Dan Lobb, Trevor Wood, “TROPOMI, the Sentinel 5 Precursor instrument for air quality and climate observations: status of the current design”, Proc. ICSO 0174 (2012).

[3] A. H. van Amerongen, H. Visser, R. J. P. Vink, T. Coppens, R. W. M. Hoogeveen., “Development of immersed diffraction grating for the TROPOMI-SWIR spectrometer”, Proc. SPIE 7826, (2010).

[4] Aaldert H. van Amerongen, Tibor Agocs, Govert Nieuwland, Hedser van Brug, Lars Venema, Ruud Hoogeveen, “Development of silicon immersed grating for METIS on E-ELT,” Proc. SPIE 8450, 8450-100 (2012).

[5] C.Grèzes-Besset, D.Torricini, F.Chazallet, “Real-time lateral optical monitoring for the production of complex multilayer stacks,” Proc. SPIE, 5963,14 (2005).